Molecular Systems Biology 8; Article number 596; doi:10.1038/msb.2012.25
Citation: ***Molecular Systems Biology*** **8:596**
© 2012 EMBO and Macmillan Publishers Limited All rights reserved 1744-4292/12
www.molecularsystemsbiology.com

molecular systems biology

The glucose-deprivation network counteracts lapatinib-induced toxicity in resistant ErbB2-positive breast cancer cells

Kakajan Komurov[1], Jen-Te Tseng[1], Melissa Muller[1], Elena G Seviour[1], Tyler J Moss[1], Lifeng Yang[2], Deepak Nagrath[2] and Prahlad T Ram[1,*]

[1] Department of Systems Biology, The University of Texas MD Anderson Cancer Center, Houston, TX, USA and [2] Chemical and Biomolecular Engineering Department, Rice University, Houston, TX, USA
* Corresponding author. Department of Systems Biology, The University of Texas MD Anderson Cancer Center, 7435 Fannin Street, Unit 0950, Houston, TX 77054, USA. Tel.: +1 713 563 4227; Fax: +1 713 563 4235; E-mail: pram@mdanderson.org

Received 2.9.11; accepted 1.6.12

Dynamic interactions between intracellular networks regulate cellular homeostasis and responses to perturbations. Targeted therapy is aimed at perturbing oncogene addiction pathways in cancer, however, development of acquired resistance to these drugs is a significant clinical problem. A network-based computational analysis of global gene expression data from matched sensitive and acquired drug-resistant cells to lapatinib, an EGFR/ErbB2 inhibitor, revealed an increased expression of the glucose deprivation response network, including glucagon signaling, glucose uptake, gluconeogenesis and unfolded protein response in the resistant cells. Importantly, the glucose deprivation response markers correlated significantly with high clinical relapse rates in ErbB2-positive breast cancer patients. Further, forcing drug-sensitive cells into glucose deprivation rendered them more resistant to lapatinib. Using a chemical genomics bioinformatics mining of the CMAP database, we identified drugs that specifically target the glucose deprivation response networks to overcome the resistant phenotype and reduced survival of resistant cells. This study implicates the chronic activation of cellular compensatory networks in response to targeted therapy and suggests novel combinations targeting signaling and metabolic networks in tumors with acquired resistance.
Molecular Systems Biology **8**: 596; published online 31 July 2012; doi:10.1038/msb.2012.25
Subject Categories: cellular metabolism; signal transduction; molecular biology of disease
Keywords: bioinformatics; computational methods; functional genomics; metabolic and regulatory networks; signal transduction

Introduction

Cellular homeostasis is maintained by dynamic interactions between networks that regulate cellular functions (Jordan *et al,* 2000). Deregulation of network dynamics caused by mutations is one of the hallmarks of cancer (Hanahan and Weinberg, 2011). The premise of oncogene addiction in cancers (Weinstein, 2002; Sharma and Settleman, 2007) suggests targeted therapy as a promising strategy in the treatment of cancer patients. Overexpression of the ERBB2/HER2 oncogenic product and increased activation of its signaling network is one of the most common events in breast cancer and correlates with poor prognosis (Slamon *et al,* 1987). Lapatinib (Tykerb, GlaxoSmithKline) is the first dual inhibitor of EGFR and ERBB2/HER2 tyrosine kinase receptors that was approved for the treatment of ErbB2-positive advanced or metastatic breast cancer patients (Medina and Goodin, 2008). Despite showing efficacy, lapatinib as a first-line monotherapy in ErbB2-positive breast cancer patients suffers from short-lived clinical responses due to acquired resistance. Recent studies examining mechanisms of resistance to lapatinib in SKBR3 and BT474 human breast cancer cells found increased expression of HER2 or HER3 (Garrett *et al,* 2011). Chronic acquired resistance to lapatinib in UACC812 cells showed a switched dependence on FGFR2 signaling (Azuma *et al,* 2011) and overexpressions of the AXL receptor tyrosine kinase (Liu *et al,* 2009) in BT474 cells. While these studies have focused on alterations at the molecular level in signaling pathways, a detailed systems-level analysis of global cellular networks altered during chronic lapatinib exposure leading to acquired resistance has not been done. Understanding the dynamic changes in cellular networks in response to perturbations leading to acquired resistance will be critical in development of novel targets or combinations of targets to overcome resistance to targeted therapy.

Results

To develop a model of acquired resistance to lapatinib, we cultured ErbB2-positive SKBR3 cells with increasing doses of

© 2012 EMBO and Macmillan Publishers Limited

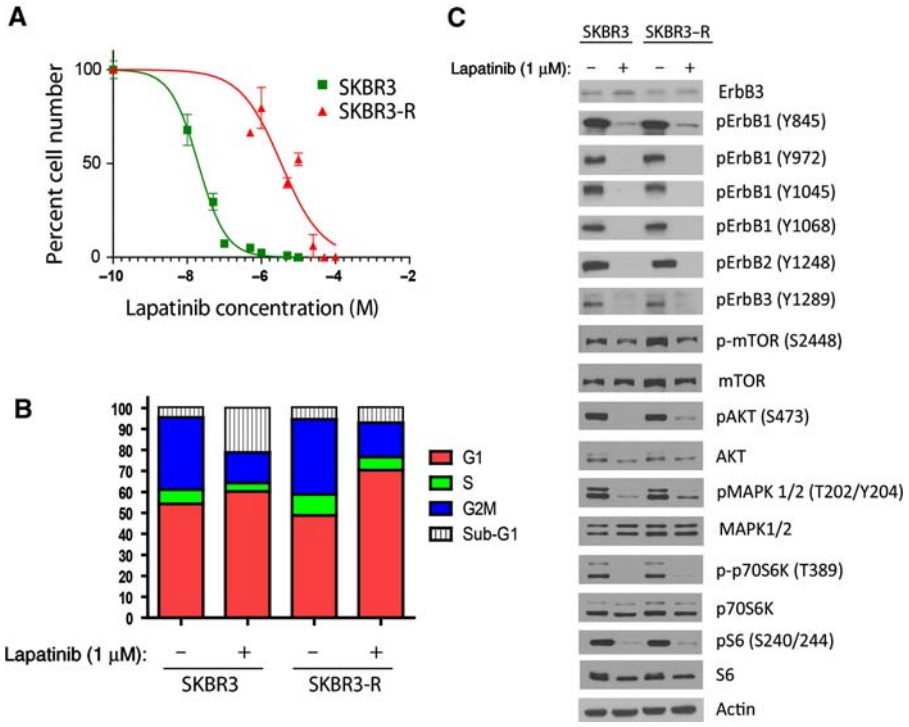

Figure 1 Initial characterization of lapatinib-resistant cell line. (**A**) Percent change in cell numbers in response to increasing doses of lapatinib in parental and resistant SKBR3 cells. (**B**) Cell-cycle and apoptosis analysis of the parental and resistant cells in response to 1 μM lapatinib after 4 days. (**C**) Immunoblotting of ErbB signaling pathway before and after 1 μM lapatinib treatment. Immunoblotting of phosphorylation sites on ErbB1, 2 and 3 family members as well as the downstream signaling proteins AKT, MAPK1, 2, mTOR, S6Kinase and S6 before and after lapatinib treatment.

lapatinib for a year, in parallel control parental cell was also cultured in normal conditions with no lapatinib. The resultant cell line variant, SKBR3-R, is almost 100-fold more resistant to lapatinib treatment when compared with the parental SKBR3 (Figure 1A). In line with previous studies, we find that lapatinib induces a significant amount of apoptosis as characterized by sub-G1 DNA content in SKBR3 but not in SKBR3-R cells (Figure 1B). Previous studies have implicated acquired mutations in EGFR/ErbB2 or overexpression of ErbB3 as a possible mechanism of lapatinib resistance. We sequenced EGFR and ErbB2 kinases and found no acquired mutations in the mutation hot spots reported for these genes (Supplementary Figure 1). We measured ErbB3 protein levels and found no increase in ErbB3 levels between parental and resistant cells (Figure 1C). However, there is a small increase in total ErbB3 levels in response to lapatinib in both parental and resistant cells as previously described (Figure 1C; Garrett *et al,* 2011). We next determined the effect of lapatinib treatment on inhibition of EGFR/ ErbB2 phosphorylation in both parental and resistant cells (Figure 1C), and found that EGFR/ErbB2/ ErbB3 phosphorylation was equally inhibited in both sensitive and resistant cells (Figure 1C).

To determine the effect of lapatinib on downstream signaling pathways from EGFR/ErbB2, we measured changes in phosphorylation of MAPK1,2, AKT, mTOR, TSC2, P70S6K and S6 and found that lapatinib equally inhibited their phosphorylation in both the parental and resistant cells (Figure 1C). We additionally genotyped the parental and resistant cells in the MDACC Characterized Cell Line Core using Sequenome analysis and compared it with the ATCC-derived SKBR3 cells to ensure the acquired resistance cells were in fact SKBR3 cells (Supplementary Figure 2). Having found no additional mutations in EGFR/ErbB2, no increase in ErbB3 and equal inhibition of EGFR/ErbB2/ErbB3 signaling between the parental and resistant cells we wanted to determine what alterations of cellular processes outside the classical EGFR/ ErbB2 pathway may contribute to acquired lapatinib resistance in breast cancer cells.

To gain insight into the global cellular processes altered during the acquired lapatinib resistance in SKBR3 cells, we measured gene expression changes in SKBR3 and SKBR3-R cells before and after treatment with 0.1 or 1 μM lapatinib for 24 h. Functional analyses of global gene expression data are enhanced by employing network-based approaches within the context of *a priori* information (Ideker *et al,* 2011). Here, in order to understand the specific network alterations contributing to acquired resistance of SKBR3-R cells to lapatinib, we employed NetWalk, a random walk-based network scoring method for genomic data analyses (Komurov *et al,* 2010). In contrast to other similar network analysis methods, NetWalk output is not a collection of networks, but rather a distribution of network-wide scores for each interaction in the network based on the local connectivity as well as the supplied gene expression values. This enables direct comparative analyses of gene expression data between different conditions at a network, rather than at a gene level. To facilitate network analyses of signaling pathways, transcriptional networks, metabolic networks and functional interactions

© 2012 EMBO and Macmillan Publishers Limited

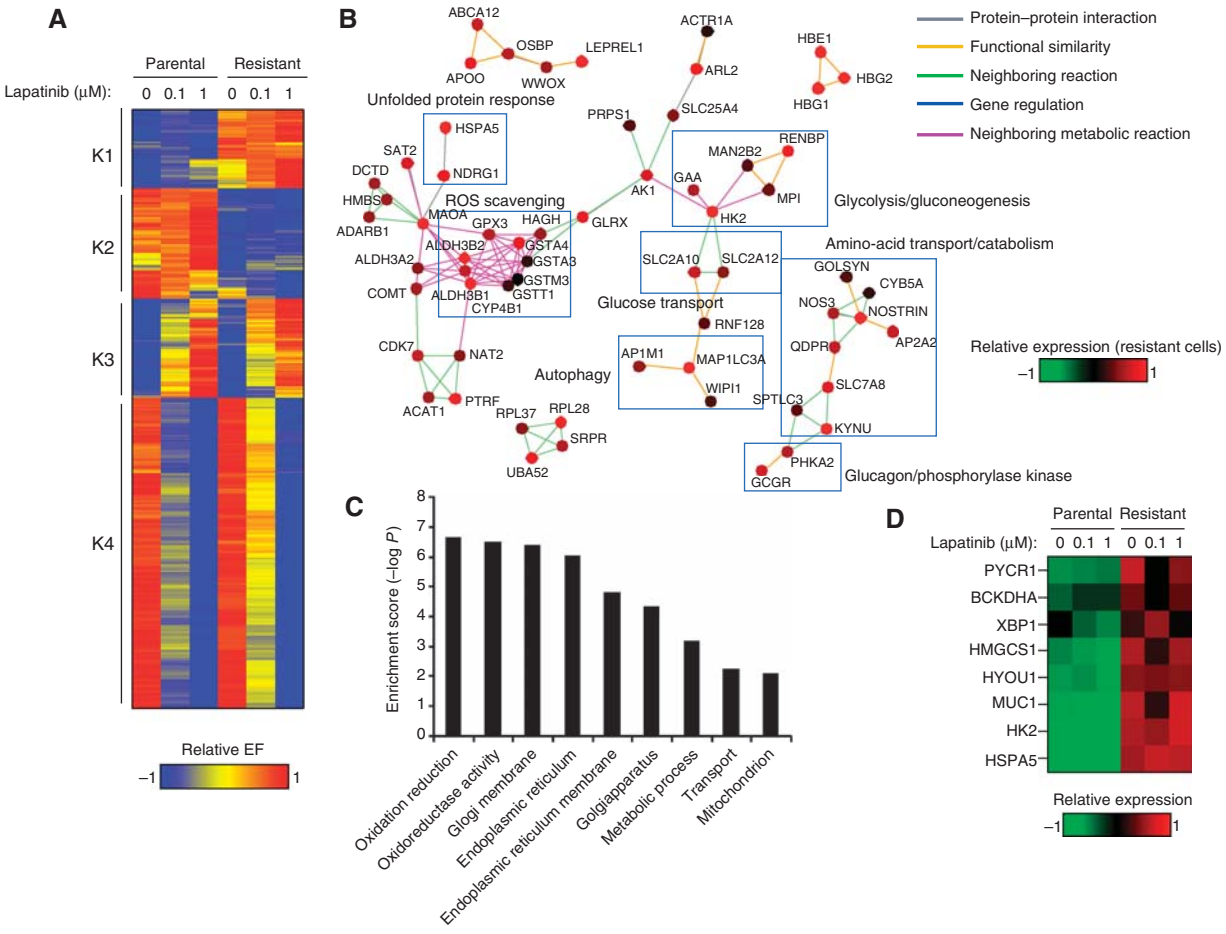

Figure 2 Network analyses of gene expression data. (**A**) A heatmap of Edge Flux (EF) values with highest variance across the six conditions (see text and Materials and methods). (**B**) A network plot of the interactions in K1. Nodes are colored by the relative gene expression values of respective genes in resistant cells (see the red-green color key), and edges are colored according to the type of interaction. (**C**) Functional enrichment scores of highest scoring GO functional classes in the network of 500 highest EF values in resistant cells relative to parental cells. Enrichment score was calculated as the − log of hypergeometric distribution function. (**D**) Heatmap of gene expressions of some genes in our data set previously implicated in glucose deprivation response.

in the gene expression data, we compiled a comprehensive network of binary relationships between genes based on physical, regulatory and neighboring interactions as well as functional similarity as cataloged in various online databases (see Materials and methods). Overall, our network accounts for ~240 000 physical and functional interactions among 15 106 unique genes.

Using the respective microarray gene expression data, we obtained Edge Flux (EF) value distribution for each condition (see Materials and methods). The heatmap of 1000 EF values with highest variance across the six conditions (0, 0.1 and 1 μM lapatinib treatment for 24 h for SKBR3 and SKBR3-R cells) is displayed in Figure 2A. The same analysis using the highest 480 values is shown in Supplementary Figure 3. Four clusters, K1 through K4, with distinct temporal expression patterns are clearly identifiable. Networks in K1 are specifically upregulated at the basal level in the resistant cells, while those in K2 are specifically downregulated in these cells. K3 contains networks that are upregulated, and K4 contains networks that are downregulated, in response to lapatinib in both cell lines. Heatmap visualization of the data without NetWalk analysis is shown in Supplementary Figure 4. Plotting of the network in K1 shows extensive upregulation in the resistant cells of the cellular processes involved in glucose uptake, glucagon signaling, unfolded protein response (UPR) and oxidation/reduction (Figure 2B). The network in K2 is primarily composed of signaling pathways involved in TGFβ signaling and inflammatory response (Supplementary Figure 5), and the network in K3 contains processes involved in oxidation/reduction, cell-cycle arrest and EGF signaling (Supplementary Figure 6). K4 almost exclusively consists of cell-cycle processes (Supplementary Figure 7). We performed GSEA analysis of the same data set and the GSEA analysis failed to identify these functionally relevant gene networks (Supplementary Figure 8). Lapatinib-mediated downregulation of cell-cycle machinery in K4 and upregulation of cell-cycle inhibitory complexes and EGF signaling in K3 in both cell lines are in line with our expectations regarding cellular responses to lapatinib, which involves cell-cycle arrest and attempts at restoring EGF signaling. However, the networks in K1 and K2, which are specifically activated and inhibited, respectively, in resistant cells, and therefore constitute the clusters of highest interest within the context of this study, have not been previously associated with

© 2012 EMBO and Macmillan Publishers Limited

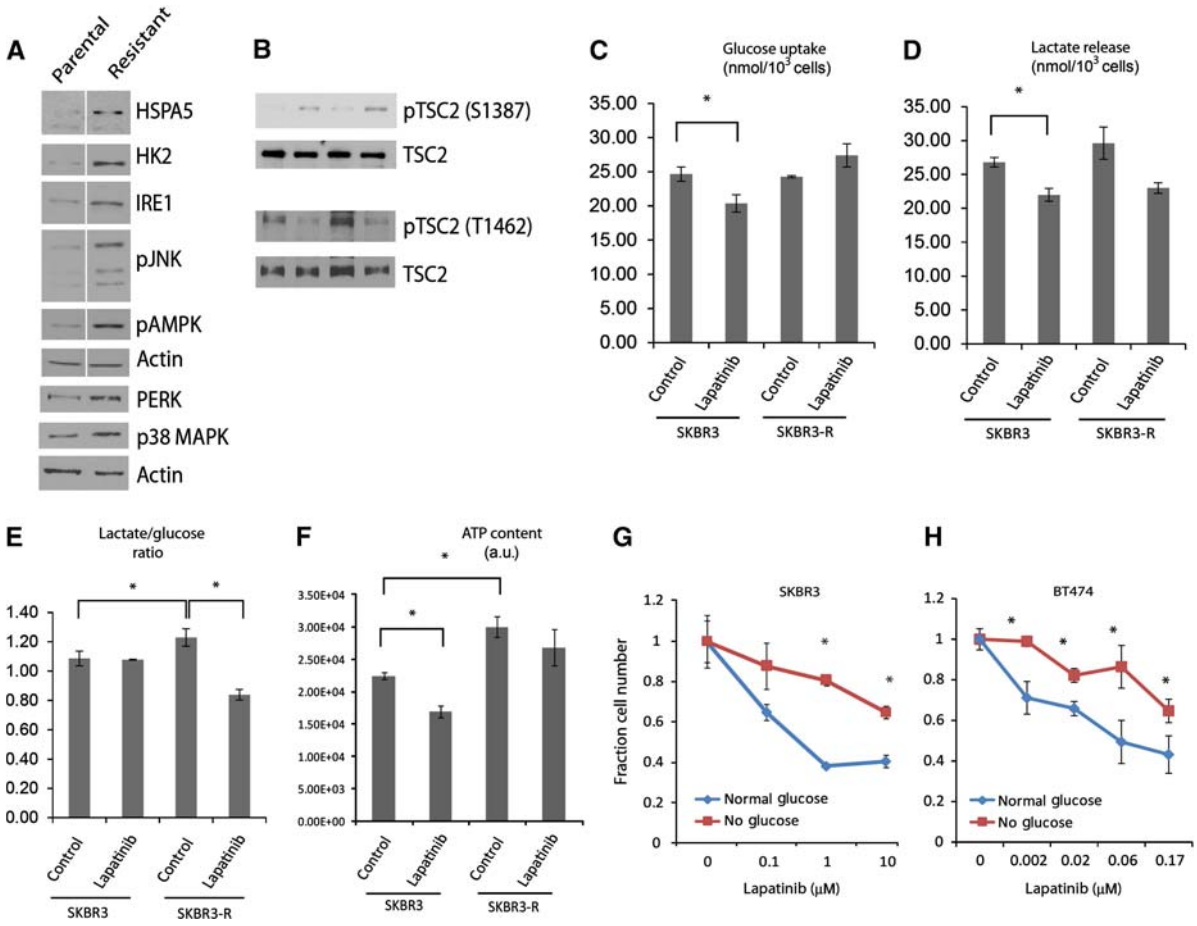

Figure 3 Glucose deprivation response phenotype in lapatinib resistance. (**A**) Immunoblotting of key members of glucose deprivation response in parental and resistant cells HSPA5, HK2, IRE1, pJNK, pAMPK, PERK and p38. (**B**) Immunoblotting of the AKT and AMPK phosphorylation sites on TSC2 in parental and resistant cells. (**C**) Glucose uptake flux analysis (*$P<0.05$), (**D**) lactate production flux analysis (*$P<0.05$), (**E**) ratio of lactate to glucose (*$P<0.05$) and (**F**) total ATP content of parental and resistant cells after 24 h of lapatinib treatment (*$P<0.01$). (**G**) Change in cell numbers of parental SKBR3 cells treated with increasing doses of lapatinib in a media with normal and no glucose (*$P<0.01$). (**H**) Change in cell numbers of BT474 cells treated with increasing doses of lapatinib after prolonged incubation in a media with normal (2 g/l) and low (0.25 g/l) glucose (*$P<0.01$).

acquired resistance to targeted therapy. Therefore, we chose to analyze these clusters in more detail.

Interestingly, processes in the K1 cluster are reminiscent of a classical glucose deprivation response, where endoplasmic reticulum (ER) stress in the form of the UPR, amino-acid catabolism, glucagon signaling, increase in the expression of glucose transporters and glycogen breakdown are common responses (Hotamisligil, 2010). Indeed, a functional enrichment analysis of the 500 highest EF values in the resistant cells relative to parental cells using hypergeometric probability distribution function shows a specific enrichment of processes associated with the ER (Figure 2C), further suggesting that networks associated with the ER and nutrient stress are upregulated in the resistant cells. Furthermore, several of the previously published markers of glucose deprivation and ER stress response markers are also upregulated in the resistant cells at the basal level relative to parental cells (Figure 2D), indicating that the resistant cells indeed display a nutrient-starved phenotype.

Western blot analysis revealed that key members of the ER stress response pathways, the ER chaperone GRP78 (glucose deprivation response protein of 78 kDa, HSPA5 gene), inositol requiring protein-1 (IRE1) and phospho-JNK, which is activated by IRE1 during ER stress (Hotamisligil, 2010), are all markedly elevated in the resistant cells (Figure 3A). Additionally, we also found an increase in p38 and PERK and in the phosphorylation of AMPK in the resistant cells (Figure 3A).

TSC2 serves as key player in the juxtaposition between signaling and metabolism and is phosphorylated by both AKT and AMPK. Phosphorylation of the TSC2 protein by AMPK is a hallmark of nutrient starvation (Inoki *et al*, 2003), and we found increased phosphorylation of TSC2 at the AMPK site (S1387) in the resistant cells at the basal level. Interestingly, lapatinib treatment increased its phosphorylation in both parental and resistant cells; however, the maximal levels were observed in the resistant cells (Figure 3B). In contrast, the AKT phosphorylation site on TSC2 (T1462) exhibited a different behavior with lapatinib blocking the phosphorylation in both parental and resistant cells similarly to the effect on the other signaling proteins (Figure 1D).

Cellular response to nutrient deprivation aims to restore glucose uptake and energy production through upregulation of the glucose transporters as well as alternative pathways of

© 2012 EMBO and Macmillan Publishers Limited

energy production through amino acid and fatty acid breakdown; while trying to minimize the damage of ROS and hypoglycosylated proteins in the ER through UPR (Hotamisligil, 2010). Since inhibition of EGF signaling in ErbB2-positive breast cancers has been associated with glucose deprivation and energetic stress (Weihua *et al,* 2008; Schafer *et al,* 2009), we hypothesized that lapatinib-mediated cell toxicity may be associated with inhibition of glucose uptake and subsequent energetic stress. Treatment of SKBR3 cells with lapatinib impaired their ability to uptake glucose from the media and perform glycolysis, while the resistant cells were not significantly affected (Figure 3C and D). Lactate-to-glucose ratio of the fluxes showed that the resistant cells had a higher glycolysis rate as compared with the parental cells (Figure 3E). Lapatinib treatment induced no change in the parental cell but there was decrease in lactate/glucose ratio in the resistant cell, suggesting a switch from glycolysis to the pentose phosphate pathway shunt. Lapatinib treatment leads to ATP depletion in the parental, but not in the resistant cells (Figure 3F). These observations suggest that lapatinib-mediated toxicity is associated with glucose starvation and energy deprivation, and that SKBR3-R cells resist this effect. Since the resistant cells were not phenotypically under glucose starvation and were not energy deprived, the elevated networks of the UPR and other hypoglycemic response pathways in these cells may be an adaptation to prolonged lapatinib treatment, giving these cells the ability to uptake and metabolize glucose independent of the EGFR/ErbB2 pathway. Indeed, forcing parental cells into hypoglycemia by incubating them in a media with no glucose rendered them more resistant to lapatinib-mediated growth inhibition (Figure 3G), indicating that cellular hypoglycemic response can confer resistance to inhibition of ErbB2 signaling. Importantly, lapatinib-induced inhibition of glucose uptake and the protective effect of hypoglycemic response was observed with another ErbB2-positive breast cancer cell line, BT474 (Figure 3H).

Large-scale clinical analyses of mRNA expression profiles of cancer patients provide an invaluable resource for testing the clinical relevance of findings from the *in-vitro* cell culture models. We asked whether our findings in the cell culture model of acquired lapatinib resistance are also manifest in the breast cancer patients *in vivo*. Unfortunately, ideal sets of data to make such an analysis possible, that is, mRNA expression profiles and clinical data of ErbB2-positive breast cancer patients treated with lapatinib, are not available. Therefore, we asked if the networks associated with lapatinib resistance in our cell culture model correlate with overall survival or relapse rates of patients with breast cancers whose tumors express high ErbB2 levels. To answer this question, we elected to employ a network approach, where we sought to construct a network of gene–gene interactions that most correlate with high relapse rates in ErbB2-positive patients. Using the breast cancer cohort data from Miller *et al* (2005), we calculated COX regression coefficients between the expression of every gene and the relapse status of patients with high ErbB2 levels (see Materials and methods). Here, a high COX coefficient indicates high correlation of the gene's expression level with poor outcome. Using the distribution of COX regression values as input to NetWalk, we obtained the network of highest scoring interactions that best correlate with high relapse rates in ErbB2-positive patients (Figure 4A). In addition to some of the previously well-characterized pathways of cell-cycle progression involved in poor outcome, this network also contains networks involved in glucose/nutrient deprivation response (see Figure 4A), which are also upregulated in our resistant cells (HK2, SLC2A10, NDRG1; Figure 4B). In contrast, while ErbB3 by itself shows a significant correlation with poor disease-free survival, most other genes in the ErbB3 network do not show the same association between their expression levels and patient outcome (Supplementary Figure 9). To identify cell processes that are most significantly associated with high relapse rates in ErbB2-positive patients, we carried out a functional enrichment analysis of the network corresponding to highest EF values calculated using the COX coefficient values above (see Materials and methods). We observed that a GO functional category 'unfolded protein binding' was one of the most highly enriched processes in this network, along with those involved in cell-cycle progression (Figure 4C), indicating that the pathways involved in UPR similar to those activated in our resistant cells are associated with poor outcome in ErbB2-positive breast cancers. Importantly, several of the markers of glucose deprivation/UPR in the network in Figure 4B were also indicative of poor prognosis in other independent breast cancer patient cohorts (Supplementary Figure 10). These correlations in the clinical data sets strongly corroborate with our findings in our cell culture models, and implicate the cellular response to glucose deprivation in the form of UPR and/or gluconeogenesis as important biological processes in the relapse of ErbB2 overexpressing breast tumors.

Finding vulnerable intervention points of tumor cells that have progressed on targeted therapies is of critical importance for designing novel therapeutic strategies for such tumors (Haber *et al,* 2011). Therefore, we asked if the activated pathways of UPR and glucose deprivation response in the resistant cells can be targeted for therapeutic purposes. To find potential drug candidates for the reversal of the glucose deprivation response phenotype in resistant cells, we employed a chemical genomics bioinformatics approach leveraging the connectivity map data set, which is a useful resource for finding drugs with novel functions based on gene expression (Lamb *et al,* 2006). We identified a set of 12 genes that are involved in the glucose deprivation response and UPR that are also upregulated in the resistant cells (see Figure 5 legend), and used this gene set to query the drugs in the CMAP data set that caused their downregulation. We scored each condition in the CMAP data set by summing the ranks (lower means downregulated) of the 12 genes, and identified 5 drugs with the lowest scores (Figure 5A). Interestingly, the drug with the second lowest score was pyrvinium, an anthelmintic drug, that has been previously shown to inhibit UPR associated with hypoglycemia and therefore specifically kill cells that are deprived of glucose (Yu *et al,* 2008; Saito *et al,* 2009). To test if downregulation of the glucose deprivation response genes by pyrvinium in the CMAP data set is statistically significant, we calculated the average ranks of 10 000 randomly selected 12 genes in the pyrvinium data set and compared with the ranks of the glucose deprivation response genes. Based on this analysis, the downregulation of the glucose deprivation

© 2012 EMBO and Macmillan Publishers Limited

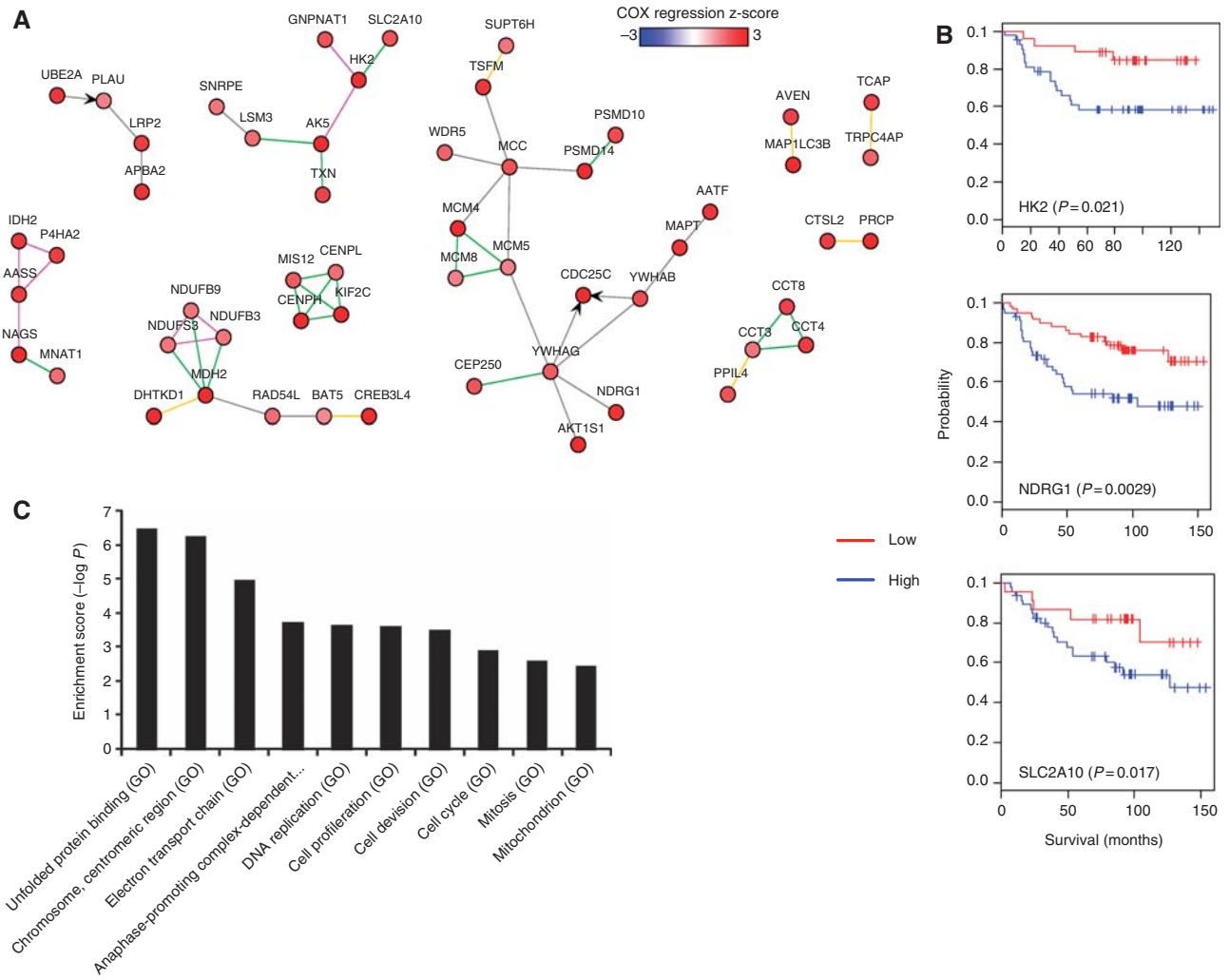

Figure 4 Correlation of glucose deprivation response with clinical relapse rates in ErbB2-positive breast cancers. (**A**) Network of genes with highest correlation with relapse in ErbB2-positive tumor patients (see Materials and methods). Node coloring reflects the strength of correlation (COX regression z-score, see color key). Edge coloring is same as in Figure 2A. (**B**) Kaplan–Meier plots of relapse-free survival of ErbB2-positive patients segregated based on their expression of some key members of glucose deprivation response in lapatinib-resistant cells that are also present in the network in Figure 4A. (**C**) Functional enrichment scores of highest scoring GO functional categories in the network of highest EF values calculated by NetWalk analysis of COX regression values. Functional enrichment scores are calculated as − log of the hypergeometric distribution function.

response genes was highly significant relative to what would be expected by chance (Figure 5B). Therefore, we asked if treatment with pyrvinium can be preferentially toxic to resistant cells, as they have a specific upregulation of the hypoglycemic response networks. Indeed, a dose–response survival assay with pyrvinium showed that lapatinib-resistant cells are significantly more sensitive to pyrvinium when compared with parental cells (Figure 5C). Importantly, the parental cells can be sensitized to pyrvinium under low-glucose conditions (Supplementary Figure 11), indicating that the toxicity of pyrvinium in resistant cells is due to elevated pathways of UPR and hypoglycemic response. We targeted UPR using Metformin which has been previously shown to target the UPR gene program (Saito *et al,* 2009) and found that Metformin significantly inhibits lapatinib-resistant cells compared with the parental cells (Supplementary Figure 12) very similar to the response to pyrvinium.

Similarly to UPR, autophagy is also a survival response to nutrient deprivation (Hotamisligil, 2010; Kroemer *et al,* 2010) and its inhibition can also be selectively toxic in nutrient-limiting conditions (Sato *et al,* 2007; Yin *et al,* 2009), especially in transformed cells (Sheen *et al,* 2011). Autophagy is activated in the resistant cells at the basal level and in parental cells in response to lapatinib (Figure 5D). Therefore, we tested if resistant cells are more sensitive to bafilomycin A, a selective inhibitor of autophagy by the virtue of its ability to inhibit vacuole maturation. Indeed, lapatinib-resistant cells were significantly more sensitive to bafilomycin A doses when compared with parental cells (Figure 5E), and parental cells could be sensitized to bafilomycin A when placed in a low-glucose media (Supplementary Figure 13). The data above show that acquired resistance of SKBR3 cells to lapatinib is associated with increased expressions of glucose deprivation and ER stress response networks, and that selective targeting

© 2012 EMBO and Macmillan Publishers Limited

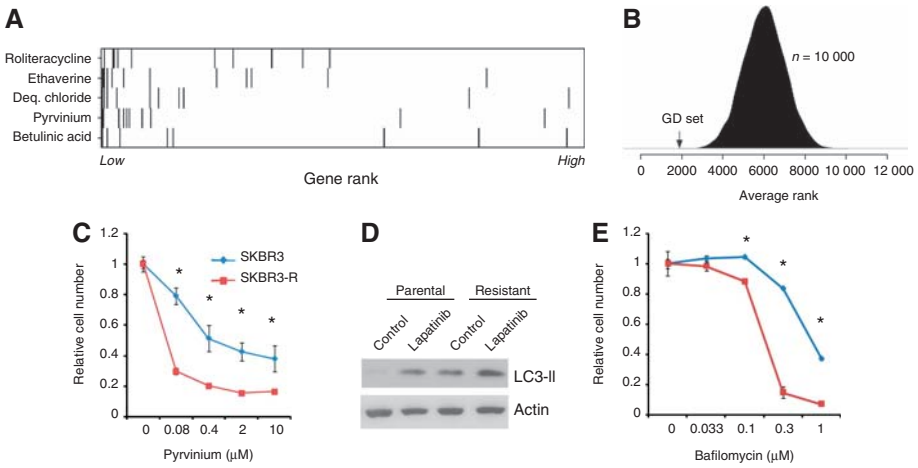

Figure 5 Identification and treatment of resistant cells with drugs reversing the hypoglycemic response phenotype. (**A**) Gene expression profiles of 12 genes in the glucose deprivation response gene set that are specifically upregulated in the resistant cells. Tested genes are HSPA5, NDRG1, HK2, SLC2A10, HYOU1, HMGCS1, SRPR, ALDH3 A2, UGCGL1, GYS1, TXNIP and GLRX. The plot shows the position of each of these genes (indicated by a black vertical line) in the whole distribution of gene expression values in response to indicated drugs. Note specific positioning of most of these genes in the lower part of the distribution with pyrvinium. (**B**) Distribution of average ranks of 10 000 random draws of 12 genes in the pyrvinium data. The arrow indicates the average rank of the GD (glucose deprivation response) set. (**C**) Change in cell numbers of the parental and resistant cells in response to increasing doses of pyrvinium after 3 days of treatment (*$P<0.01$). (**D**) Western blots of parental and resistant cells before and after treatment with lapatinib probed for LC3-II, a lipidated LC3 molecule, a marker of active autophagy. (**E**) Change in cell numbers of the parental and resistant cells in response to increasing doses of bafilomycin A (*$P<0.01$).

of these processes can be an effective therapeutic strategy against these tumors.

Discussion

Targeted therapy exploiting vulnerabilities of tumor cells to the inhibition of driver oncogenes has a premise of higher efficacy and lower toxicity in the clinic (Weinstein, 2002; Sharma and Settleman, 2007; Haber *et al,* 2011). However, the initial dramatic response in the clinic to these targeted drugs is almost inevitably followed by tumor relapse due to acquired resistance. Although some of the cases of acquired resistance are associated with the acquisition of novel mutations rendering the target oncogene insensitive to the inhibitory effects of the drug (Kobayashi *et al,* 2005; Talpaz *et al,* 2006), others involve activation of compensatory pathways (Engelman *et al,* 2007; Chen *et al,* 2008; Liu *et al,* 2009; Azuma *et al,* 2011), possibly through epigenetic reprogramming (Sharma *et al,* 2010). Finding new vulnerabilities, or targetable new *addictions*, of these tumors is an area of active investigation and constitutes a priority in cancer research.

We found that lapatinib-induced toxicity of ErbB2-positive cells is associated with glucose deprivation, and that prolonged lapatinib treatment can lead to acquired resistance that is characterized by increased expression of networks involved in glucose deprivation or hypoglycemic response. The compensatory upregulation of the glucose deprivation response networks presumably provides EGFR/ErbB2-independent mechanism of glucose uptake and survival, which confers resistance to small molecule inhibition of these receptors. Importantly, our observations suggest that addiction of ErbB2-positive cells on EGFR/ErbB2 signaling may be due to increased demand for glucose uptake in these tumor cells that is largely dependent on EGFR/ErbB2 signaling. Although this hypothesis may seem in contrast to the popular view that increased ErbB2 signaling is required to counter pro-apoptotic signals, it is in line with a recent study implicating the cellular capacity for glucose uptake as a major driving factor for oncogenic mutations (Yun *et al,* 2009), and newly emerging paradigm of cancer cell metabolism (Vander Heiden *et al,* 2009). Our data show that lapatinib-resistant cells are dependent on UPR and autophagy for survival, much like cells in hypoglycemic environments, which are also selectively sensitive to inhibitors of UPR and autophagy (Yu *et al,* 2008; Saito *et al,* 2009). Lapatinib-resistant cells have higher glycolysis rates based on the lactate-to-glucose flux ratio as compared with the parental cells, suggesting increased glucose utilization in line with the gene network changes present in these cells. The addition of lapatinib does not alter the lactate-to-glucose flux ratio in the parental cells but significantly decreases the ratio in resistant cells, suggesting a switch from glycolysis to the pentose phosphate pathway shunt that results in increased NADPH and increased ability of the cell to overcome reactive oxidative stress. Since lapatinib-resistant cells have chronically activated glucose deprivation response pathways, it is possible that increased levels of UPR and autophagy in these cells are required to counter death-promoting stress signals associated with cellular program of nutrient starvation response. Nevertheless, our observations reveal a specific dependence of lapatinib-resistant cells on the nutrient starvation response program that can be exploited therapeutically.

Analysis of ErbB2-positive patient data showed strong correlations of disease-free survival with the upregulation of glucose deprivation response networks, linking our cell line model with clinical data. Similar high correlations were also observed with ErbB3 and AXL expression, two previously identified mediators of lapatinib resistance (Engelman *et al,* 2007; Liu *et al,* 2009; Garrett *et al,* 2011), with poor disease-free survival, thereby suggesting that both signaling and metabolic changes may be associated with lapatinib resistance in breast

© 2012 EMBO and Macmillan Publishers Limited

cancer. Our work here and recent data from others suggest that reconstituting the metabolic demand of tumor cells is a major factor driving specific regulatory network rearrangements during acquired resistance to targeted therapy, and that targeting these compensatory networks may be an effective strategy against tumors with acquired resistance.

Materials and methods

Cell lines and reagents

SKBR3 breast cancer cell line was obtained from UT MD Anderson Cancer Center Characterized Cell Line Core Services. Both SKBR3 and SKBR3-R cell lines were characterized by the MDACC CCSG Characterized Cell Line Core using Sequenome analysis and found to be related to ATCC-derived SKBR3 and known mutation sites on EGFR/ErbB2 sequenced (Supplementary Figures 1 and 2). Cells were routinely maintained in RPMI-1640 (Invitrogen, Carlsbad, CA, USA) supplemented with 10% fetal bovine serum (FBS; Sigma-Aldrich, St Louis, MO, USA) and penicillin/streptomycin (Mediatech, Manassas, VA, USA). Lapatinib (LC Laboratories, Woburn, MA, USA) was dissolved in dimethyl sulfoxide (DMSO). Glucagon Receptor antagonist was purchased from EMD Biochemicals. Pyrvinium pamoate, Bafilomycin and metformin were purchased from Sigma.

Microarray experiments

Cells were treated with Lapatinib as indicated. After 24 h of treatment, cells were lysed and total RNA was extracted using Ambion mirVana miRNA Isolation Kit (Applied Biosystems) and amplified using Illumina Totalprep RNA Amplification Kit (Applied Biosystems), according to manufacturer's protocol. Equal amounts of RNA from each sample were loaded onto HumanHT-12 Expression BeadChip (Illumina, San Diego, CA, USA). The chips were hybridized for 16 h at 58°C and were scanned by UT Health Science Center Houston Microarray Services. Gene array data were analyzed using BeadStudio by Illumina. The microarray experiment was done using three independent repeats of each condition and performed at two different times.

Data availability

The gene microarray data discussed in the publication have been deposited in NCBI's Gene Expression Omnibus and are accessible through GEO Series accession number GSE38376 (http://www.ncbi.nlm.nih.gov/geo/query/acc.cgi?acc=GSE38376)

FACS analyses

Cells were treated as indicated, trypsinized, resuspended in medium, and centrifuged at 200 *g* for 6 min twice. Cells were single-cell resuspended in PBS (1×10^6 to 10^7 cells in 0.5 ml). Cell mixture was added to 4.5 ml of 70% ethanol for fixation and incubated at 4°C (2 h minimum). Samples were resuspended in 5 ml PBS, centrifuged after which supernatant was decanted. The cells were incubated in 1 ml propidium iodide staining solution (0.1% (v/v) Triton X-100 in PBS, 0.2 mg/ml RNase A, 0.02 mg/ml propidium iodide) at room temperature for 30 min. Cell fluorescence was measured by flow cytometry. For each sample, 20 000 cells were scanned. Analyses of data were performed using DNA content histogram deconvolution software Cell Quest Pro.

Crystal violet assay for determining cell density

Cells were stimulated in 96-well plates as indicated. At the time of the assay, media in the wells was dumped, and a volume of 50 µl of crystal violet solution (0.5% crystal violet (w/v), 20% methanol (v/v)) was added to each well to allow staining for 10 min, followed by gentle rinse with water to remove excess stain. Once dried, the wells were filled with 100 µl of sorensins buffer (0.1 M sodium citrate (pH 4.2), 50% (v/v) ethanol) to redissolve crystal. Cell density was determined by measuring the absorbance at 570 nm using a Vmax kinetic microplate reader (Molecular Devices, Sunnyvale, CA, USA).

Metabolic assays

Glucose uptake assay

Glucose uptake assay was performed using Wako Glucose kit according to manufacturer's protocol 2 days after treatment with lapatinib or vehicle control. Briefly, 2 µl sample was injected into 250 µl reconstituted Wako glucose reagent in a 96-well plate, mixed thoroughly, and incubated at 37°C for 5 min. The absorbance was measured at 505 nm using a spectrophotometer (SpectraMax M5 from Molecular Devices) and the difference of absorbance between the spent media and control media indicated the glucose uptake of cells. Cells were counted in each of the wells and the media was changed every 24 h to calculate glucose flux per cell per day.

Lactate secretion

Lactate secretion was determined using Trinity Lactate Kit according to manufacturer's protocol 2 days after treatment with lapatinib or vehicle control. Briefly, lactate reagent was reconstituted with 10 ml milliohm water and diluted 1:4 in 0.1 M Tris solution (pH 7.0). Media samples were diluted 1:10 in PBS and lactate reagent was added to the diluted samples in an assay plate. The plate was protected from light and incubated for 1 h before reading the change in absorbance on a spectrophotometer at 540 nm. Cells were counted in each of the wells and the media was changed every 24 h to calculate lactate flux per cell per day.

ATP measurement

Cellular ATP was determined by ATPlite 1-step (Perkin-Elmer) according to manufacturer's protocol. To control for cell density between different treatments, final readings were divided by Crystal Violet readings of wells growing cells under identical conditions.

SDS–PAGE and immunoblotting

Cells were lysed by incubation on ice for 15 min in a sample lysis buffer (50 mM Hepes, 150 mM NaCl, 1 mM EGTA, 10 mM Sodium Pyrophosphate, pH 7.4, 100 nM NaF, 1.5 mM $MgCl_2$, 10% glycerol, 1% Triton X-100 plus protease inhibitors; aprotinin, bestatin, leupeptin, E-64 and pepstatin A). Cell lysates were centrifuged at 15 000 *g* for 20 min at 4°C. The supernatant was frozen and stored at −20°C. Protein concentrations were determined using a protein-assay system (Bio-Rad, Hercules, CA, USA), with BSA as a standard. For immunoblotting, proteins (25 µg) were separated by SDS–PAGE and transferred onto Hybond-C membrane (GE Healthcare, Piscataway, NJ, USA). Blots were blocked for 60 min and incubated with primary antibodies overnight, followed by goat anti-mouse IgG-HRP (1:30 000; Cell Signaling Technology, Boston, MA, USA) or goat anti-rabbit IgG-HRP (1:10 000; Cell Signaling Technology) for 1 h. Secondary antibodies were detected by enhanced chemiluminescence (ECL) reagent (GE Healthcare).

Antibodies

All the antibodies were from Cell Signaling, except for GCGR (Abcam) and Actin (Sigma).

Network analyses

NetWalk analyses

NetWalk is a biased random walk model for scoring each interaction in the global network of biological relationships based on combined assessment of the network connectivity and the input data (i.e., microarray gene expression data; Komurov *et al*, 2010). Essentially,

© 2012 EMBO and Macmillan Publishers Limited

NetWalk converts a gene-centric data distribution (i.e., gene expression data) to an interaction-centric distribution (EF values, see Komurov *et al,* 2010).

For the clustering in Figure 2A, the gene expression matrix containing measured gene expression values for each gene under each condition (0, 0.1 and 1 μM lapatinib treatment for parental and resistant cells at 24 h) was row-normalized by dividing the value for each gene by the mean of expression for that gene in all conditions. Then, using these values as input into NetWalk, EF values for each condition were obtained. In all, 1000 EF values with highest variance across the 6 conditions were selected for the clustering analysis in Figure 2A.

For the network in Figure 4A, the breast cancer patient cohort data set from Miller *et al* (2005) was used. COX regression z-scores and *P*-values for each gene in the data set were calculated using respective functions in the 'survival' package for R. The *z*-scores (after transformation) were used as input to NetWalk to obtain highest scoring 500 EF values. Genes in the resultant network were filtered to only include those whose COX regression *P*-values were <0.05, and genes with no interactions in the resultant network were discarded. Analysis of additional data sets UNC (https://genome.unc.edu/pubsup/breastGEO/) and IJB (Loi *et al,* 2007) was performed (Supplementary Figure 10).

Global network of biomolecular relationships

The network of protein–protein, signaling, gene regulation and functional similarity relationships was described earlier (Komurov *et al,* 2010). In order to account for molecular relationships between genes in metabolic pathways, interactions were assigned to pairs of genes if the metabolic reactions performed by their respective protein products shared a metabolite. For the latter, common metabolites such as water, ATP, ADP and phosphate were not considered. In addition, neighboring interactions from Reactome (Joshi-Tope *et al,* 2005) were also imported. This resulted in a network of 15 106 genes connected by ~240 000 interactions.

Supplementary information

Supplementary information is available at the *Molecular Systems Biology* website (www.nature.com/msb).

Acknowledgements

This work was supported in parts by a Komen for the Cure postdoctoral fellowship KG101547 to KK and NIH-R01 CA125109 to PTR. We thank Dr Ju-Seog Lee and Sang Bae Kim for help with the microarray.

Author contributions: KK, JT-T, MM, EGS, TJS, and LY performed the experiments; KK, MM, DN and PTR analyzed the data; KK and PTR wrote the manuscript.

Conflict of Interest

The authors declare that they have no conflict of interest.

References

Azuma K, Tsurutani J, Sakai K, Kaneda H, Fujisaka Y, Takeda M, Watatani M, Arao T, Satoh T, Okamoto I, Kurata T, Nishio K, Nakagawa K (2011) Switching addictions between HER2 and FGFR2 in HER2-positive breast tumor cells: FGFR2 as a potential target for salvage after lapatinib failure. *Biochem Biophys Res Commun* **407:** 219–224

Chen FL, Xia W, Spector NL (200) Acquired resistance to small molecule ErbB2 tyrosine kinase inhibitors. *Clin Cancer Res* **14:** 6730–6734

Engelman JA, Zejnullahu K, Mitsudomi T, Song Y, Hyland C, Park JO, Lindeman N, Gale CM, Zhao X, Christensen J, Kosaka T, Holmes AJ, Rogers AM, Cappuzzo F, Mok T, Lee C, Johnson BE, Cantley LC, Jänne PA (2007) MET amplification leads to gefitinib resistance in lung cancer by activating ERBB3 signaling. *Science* **316:** 1039–1043

Garrett JT, Olivares MG, Rinehart C, Granja-Ingram ND, Sánchez V, Chakrabarty A, Dave B, Cook RS, Pao W, McKinely E, Manning HC, Chang J, Arteaga CL (2011) Transcriptional and posttranslational up-regulation of HER3 (ErbB3) compensates for inhibition of the HER2 tyrosine kinase. *Proc Natl Acad Sci USA* **108:** 5021–5026

Haber DA, Gray NS, Baselga J (2011) The evolving war on cancer. *Cell* **145:** 19–24

Hanahan D, Weinberg RA (2011) Hallmarks of cancer: the next generation. *Cell* **144:** 646–674

Hotamisligil GS (2010) Endoplasmic reticulum stress and the inflammatory basis of metabolic disease. *Cell* **140:** 900–917

Ideker T, Dutkowski J, Hood L (2011) Boosting signal-to-noise in complex biology: prior knowledge is power. *Cell* **144:** 860–863

Inoki K, Zhu T, Guan KL (2003) TSC2 mediates cellular energy response to control cell growth and survival. *Cell* **115:** 577–590

Jordan JD, Landau EM, Iyengar R (2000) Signaling networks: the origins of cellular multitasking. *Cell* **103:** 193–200

Joshi-Tope G, Gillespie M, Vastrik I, D'Eustachio P, Schmidt E, de Bono B, Jassal B, Gopinath GR, Wu GR, Matthews L, Lewis S, Birney E, Stein L (2005) Reactome: a knowledgebase of biological pathways. *Nucleic Acids Res* **33**(Database issue)**:** D428–D432

Kobayashi S, Boggon TJ, Boggon TJ, Dayaram T, Jänne PA, Kocher O, Meyerson M, Johnson BE, Eck MJ, Tenen DG, Halmos B (2005) EGFR mutation and resistance of non-small-cell lung cancer to gefitinib. *N Engl J Med* **352:** 786–792

Komurov K, White MA, Ram PT (2010) Use of data-biased random walks on graphs for the retrieval of context-specific networks from genomic data. *PLoS Comput Biol* **6:** e1000889

Kroemer G, Marino G, Levine B (2010) Autophagy and the integrated stress response. *Mol Cell* **40:** 280–293

Lamb J, Crawford ED, Peck D, Modell JW, Blat IC, Wrobel MJ, Lerner J, Brunet JP, Subramanian A, Ross KN, Reich M, Hieronymus H, Wei G, Armstrong SA, Haggarty SJ, Clemons PA, Wei R, Carr SA, Lander ES, Golub TR (2006) The Connectivity Map: using gene-expression signatures to connect small molecules, genes, and disease. *Science* **313:** 1929–1935

Liu L, Greger J, Shi H, Liu Y, Greshock J, Annan R, Halsey W, Sathe GM, Martin AM, Gilmer TM (2009) Novel mechanism of lapatinib resistance in HER2-positive breast tumor cells: activation of AXL. *Cancer Res* **69:** 6871–6878

Loi S, Haibe-Kains B, Desmedt C, Lallemand F, Tutt AM, Gillet C, Ellis P, Harris A, Bergh J, Foekens JA, Klijn JG, Larsimont D, Buyse M, Bontempi G, Delorenzi M, Piccart MJ, Sotiriou C (2007) Definition of clinically distinct molecular subtypes in estrogen receptor-positive breast carcinomas through genomic grade. *J Clin Oncol* **25:** 1239–1246

Medina PJ, Goodin S (2008) Lapatinib: a dual inhibitor of human epidermal growth factor receptor tyrosine kinases. *Clin Ther* **30:** 1426–1447

Miller LD, Smeds J, George J, Vega VB, Vergara L, Ploner A, Pawitan Y, Hall P, Klaar S, Liu ET, Bergh J (2005) An expression signature for p53 status in human breast cancer predicts mutation status, transcriptional effects, and patient survival. *Proc Natl Acad Sci USA* **102:** 13550–13555

Saito S, Furuno A, Sakurai J, Sakamoto A, Park HR, Shin-Ya K, Tsuruo T, Tomida A (2009) Chemical genomics identifies the unfolded protein response as a target for selective cancer cell killing during glucose deprivation. *Cancer Res* **69:** 4225–4234

Sato K, Tsuchihara K, Fujii S, Sugiyama M, Goya T, Atomi Y, Ueno T, Ochiai A, Esumi H (2007) Autophagy is activated in colorectal cancer cells and contributes to the tolerance to nutrient deprivation. *Cancer Res* **67:** 9677–9684

Schafer ZT, Grassian AR, Song L, Jiang Z, Gerhart-Hines Z, Irie HY, Gao S, Puigserver P, Brugge JS (2009) Antioxidant and oncogene rescue of metabolic defects caused by loss of matrix attachment. *Nature* **461:** 109–113

© 2012 EMBO and Macmillan Publishers Limited

Sharma SV, Lee DY, Li B, Quinlan MP, Takahashi F, Maheswaran S, McDermott U, Azizian N, Zou L, Fischbach MA, Wong KK, Brandstetter K, Wittner B, Ramaswamy S, Classon M, Settleman J (2010) A chromatin-mediated reversible drug-tolerant state in cancer cell subpopulations. *Cell* **141:** 69–80

Sharma SV, Settleman J (2007) Oncogene addiction: setting the stage for molecularly targeted cancer therapy. *Genes Dev* **21:** 3214–3231

Sheen JH, Zoncu R, Kim D, Sabatini DM (2011) Defective regulation of autophagy upon leucine deprivation reveals a targetable liability of human melanoma cells *in vitro* and *in vivo*. *Cancer Cell* **19:** 613–628

Slamon DJ, Clark GM, Wong SG, Levin WJ, Ullrich A, McGuire WL (1987) Human breast cancer: correlation of relapse and survival with amplification of the HER-2/neu oncogene. *Science* **235:** 177–182

Talpaz M, Shah NP, Kantarjian H, Donato N, Nicoll J, Paquette R, Cortes J, O'Brien S, Nicaise C, Bleickardt E, Blackwood-Chirchir MA, Iyer V, Chen TT, Huang F, Decillis AP, Sawyers CL (2006) Dasatinib in imatinib-resistant Philadelphia chromosome-positive leukemias. *N Engl J Med* **354:** 2531–2541

Vander Heiden MG, Cantley LC, Thompson CB (2009) Understanding the Warburg effect: the metabolic requirements of cell proliferation. *Science* **324:** 1029–1033

Weihua Z, Tsan R, Huang WC, Wu Q, Chiu CH, Fidler IJ, Hung MC (2008) Survival of cancer cells is maintained by EGFR independent of its kinase activity. *Cancer Cell* **13:** 385–393

Weinstein IB (2002) Cancer. Addiction to oncogenes–the Achilles heal of cancer. *Science* **297:** 63–64

Yin L, Kharbanda S, Kufe D (2009) MUC1 oncoprotein promotes autophagy in a survival response to glucose deprivation. *Int J Oncol* **34:** 1691–1699

Yu DH, Macdonald J, Liu G, Lee AS, Ly M, Davis T, Ke N, Zhou D, Wong-Staal F, Li QX (2008) Pyrvinium targets the unfolded protein response to hypoglycemia and its anti-tumor activity is enhanced by combination therapy. *PLoS One* **3:** e3951

Yun J, Rago C, Cheong I, Pagliarini R, Angenendt P, Rajagopalan H, Schmidt K, Willson JK, Markowitz S, Zhou S, Diaz Jr LA, Velculescu VE, Lengauer C, Kinzler KW, Vogelstein B, Papadopoulos N (2009) Glucose deprivation contributes to the development of KRAS pathway mutations in tumor cells. *Science* **325:** 1555–1559

SOME RIGHTS RESERVED *Molecular Systems Biology* is an open-access journal published by *European Molecular Biology Organization* and *Nature Publishing Group*. This work is licensed under a Creative Commons Attribution-Noncommercial-Share Alike 3.0 Unported License.

 © 2012 EMBO and Macmillan Publishers Limited